

Scientific paper

Synthesis, Biological Evaluation, and Molecular Docking Studies of Hydrazones as Novel Xanthine Oxidase Inhibitors

Ling-Wei Xue,^{1,*} Shi-Tong Li,² Yong-Jun Han¹ and Xiao-Qiang Luo¹¹ School of Chemical and Environmental Engineering, Pingdingshan University, Pingdingshan Henan 467000, P. R. China² Department of Materials, School of Natural Sciences, The University of Manchester, Manchester M13 9PL, United Kingdom

* Corresponding author: E-mail: pdsuchemistry@163.com

Received: 11-02-2021

Abstract

A series of hydrazones, 2-cyano-*N*'-(4-diethylamino-2-hydroxybenzylidene)acetohydrazide (**1**), *N*'-(5-bromo-2-hydroxy-3-methoxybenzylidene)-3-chlorobenzohydrazide monohydrate (**2·H₂O**), *N*'-(2-hydroxy-3-methylbenzylidene)-4-nitrobenzohydrazide (**3**), and *N*'-(2-hydroxy-3-trifluoromethoxybenzylidene)-4-nitrobenzohydrazide (**4**), were prepared and structurally characterized by elemental analysis, IR and ¹H NMR spectra, and single crystal X-ray determination. Xanthine oxidase inhibitory activities of the compounds were studied. Among the compounds, 2-cyano-*N*'-(4-diethylamino-2-hydroxybenzylidene)acetohydrazide shows the most effective activity. Docking simulation was performed to insert the compounds into the crystal structure of xanthine oxidase at the active site to investigate the probable binding modes.

Keywords: Hydrazone; xanthine oxidase; inhibition; crystal structure; molecular docking study.

1. Introduction

Enzyme inhibitors can interact with enzymes and block their activity towards natural substrates. The importance of enzyme inhibitors as drugs is enormous since these molecules have been used for treating a number of pathophysiological conditions.¹ Xanthine oxidase (XO; EC 1.17.3.2), a molybdenum hydroxylase, catalyses the hydroxylation of hypoxanthine and xanthine to yield uric acid and superoxide anions. These superoxide anions have been linked to post ischaemic tissue injury and edema as well as to vascular permeability.² XO can oxidize synthetic purine drugs, such as antileukaemic 6-mercaptopurine, with the loss of their pharmacological properties. XO has also been linked to conditions such as hepatic and kidney damage, atherosclerosis, chronic heart failure, hypertension and sickle-cell disease due to the production of reactive oxygen species (ROS) alongside uric acid.³ Then, control of the action of XO may help the therapy of some diseases. Nowadays, the treatment of gout makes use of allopurinol, a potent inhibitor of XO known for a long time.⁴ The mode of action of allopurinol involves the direct coordination of its active metabolite, oxypurinol (al-

loxanthine), to the molybdenum centre in the active site of the enzyme.⁵ However, given its side effects, toxicity, and its inability to prevent the formation of free radicals by the enzyme,⁶ the research on new XO inhibitors is needed. A number of compounds with various types like carboxylic acids and pyrimidines,⁷ pyrimidinones and 3-cyano indoles,⁸ amides,⁹ pyrazoles,¹⁰ thiobarbiturates,¹¹ hydrozingerones,¹² have been reported with XO inhibitory activities. Schiff bases have been of great interest in biological chemistry for a long time.¹³ Leigh and co-workers have reported some Schiff bases as novel XO inhibitors.¹⁴ However, the study on hydrazones is limited, and no rational structure-activity relationships have been achieved so far. As an extension of the work on the exploration of effective XO inhibitors related to Schiff bases, in this paper, a series of hydrazone type Schiff bases, 2-cyano-*N*'-(4-diethylamino-2-hydroxybenzylidene)acetohydrazide (**1**), *N*'-(5-bromo-2-hydroxy-3-methoxybenzylidene)-3-chlorobenzohydrazide monohydrate (**2·H₂O**), *N*'-(2-hydroxy-3-methylbenzylidene)-4-nitrobenzohydrazide (**3**), and *N*'-(2-hydroxy-3-trifluoromethoxybenzylidene)-4-nitrobenzohydrazide (**4**), were synthesized and structurally characterized. The XO inhibitory activities of the com-

pounds were investigated from both experimental and molecular docking study.

2. Experimental

2.1. Materials and Methods

Starting materials, reagents and solvents with AR grade were purchased from commercial suppliers and used without further purification. Elemental analyses were performed on a Perkin-Elmer 240C elemental analyzer. IR spectra were recorded on a Jasco FT/IR-4000 spectrometer as KBr pellets in the 4000–400 cm^{-1} region. ^1H NMR data were recorded on a Bruker 300 MHz instrument. X-ray diffraction was carried out on a Bruker SMART 1000 CCD area diffractometer.

2.2. General Method for the Synthesis of the Compounds

The compounds were prepared according to the literature method.¹⁵ Equimolar quantities (1.0 mmol each) of hydrazide and aldehyde were dissolved in methanol (30 mL) and stirred at room temperature for 30 min to give clear solution. X-ray quality single crystals were formed by slow evaporation of the solution in air for a few days.

2-Cyano-*N'*-(4-diethylamino-2-hydroxybenzylidene)acetohydrazide (1)

Yield: 0.22 g (82%). Mp 133–135 °C, IR (KBr, cm^{-1}) ν 3195, 3143, 2066, 1649, 1466, 1395, 1323, 1264, 1127, 1074, 963, 859, 820, 748, 520. ^1H NMR (300 MHz, DMSO- d_6) δ 10.97 (s, 1H, OH), 9.70 (s, 1H, NH), 9.62 (s, 1H, CH=N), 7.41 (d, 1H, $J = 9.0$ Hz, ArH), 6.25 (d, 1H, $J = 9.0$ Hz, ArH), 6.24 (s, 1H, ArH), 3.42 (m, 4H, CH_2), 3.33 (s, 2H, CH_2), 1.15 (t, 6H, $J = 6.0$ Hz, CH_3). Anal. Calcd for $\text{C}_{14}\text{H}_{18}\text{N}_4\text{O}_2$: C, 61.3; H, 6.6; N, 20.4; Found: C, 61.1; H, 6.7; N, 20.5%.

N'-(5-Bromo-2-hydroxy-3-methoxybenzylidene)-3-chlorobenzohydrazide monohydrate (2·H₂O)

Yield: 0.37 g (93%). Mp 221–223 °C, IR (KBr, cm^{-1}) ν 3430, 3195, 1668, 1629, 1518, 1401, 1342, 1244, 1127, 1081, 781, 709, 520. ^1H NMR (300 MHz, DMSO- d_6) δ 12.20 (s, 1H, OH), 11.72 (s, 1H, NH), 8.64 (s, 1H, CH=N), 8.02 (s, 1H, ArH), 7.87 (d, 1H, $J = 9.0$ Hz, ArH), 7.68 (d, 1H, $J = 9.0$ Hz, ArH), 7.56 (t, 1H, $J = 9.0$ Hz, ArH), 7.41 (s, 1H, ArH), 7.19 (s, 1H, ArH), 3.83 (s, 3H, CH_3). Anal. Calcd for $\text{C}_{15}\text{H}_{14}\text{BrClN}_2\text{O}_4$: C, 44.9; H, 3.5; N, 7.0; Found: C, 44.7; H, 3.6; N, 6.8%.

N'-(2-Hydroxy-3-methylbenzylidene)-4-nitrobenzohydrazide (3)

Yield: 0.26 g (86%). Mp 252–253 °C, IR (KBr, cm^{-1}) ν 3435, 3228, 1651, 1605, 1554, 1519, 1341, 1287, 1075, 853, 713, 627. ^1H NMR (300 MHz, DMSO- d_6) δ 12.67 (s, 1H, OH), 11.83 (s, 1H, NH), 8.60 (s, 1H, CH=N), 8.40 (d,

2H, $J = 8.6$ Hz, ArH), 8.19 (d, 2H, $J = 8.6$ Hz, ArH), 7.32 (d, 1H, $J = 7.6$ Hz, ArH), 7.25 (d, 1H, $J = 7.2$ Hz, ArH), 6.88 (t, 1H, $J = 7.5$ Hz, ArH), 2.23 (s, 3H, CH_3). Anal. Calcd for $\text{C}_{15}\text{H}_{13}\text{N}_3\text{O}_4$: C, 60.2; H, 4.4; N, 14.0. Found: C, 60.4; H, 4.3; N, 14.0%.

N'-(2-Hydroxy-3-trifluoromethoxybenzylidene)-4-nitrobenzohydrazide (4)

Yield: 0.33 g (89%). Mp 245–247 °C, IR (KBr, cm^{-1}) ν 3434, 3112, 1648, 1536, 1401, 1255, 1160, 1115, 1040, 862, 785, 710, 670. ^1H NMR (300 MHz, DMSO- d_6) δ 12.15 (s, 1H, OH), 12.01 (s, 1H, NH), 8.71 (s, 1H, CH=N), 8.39 (d, 2H, $J = 8.6$ Hz, ArH), 8.18 (d, 2H, $J = 8.5$ Hz, ArH), 7.67 (s, 1H, ArH), 7.33 (d, 1H, $J = 9.0$ Hz, ArH), 7.03 (d, 1H, $J = 8.9$ Hz, ArH). Anal. Calcd for $\text{C}_{15}\text{H}_{10}\text{F}_3\text{N}_3\text{O}_5$: C, 48.8; H, 2.7; N, 11.4. Found: C, 48.7; H, 2.9; N, 11.5%.

2.3. Measurement of the XO Inhibitory Activity

The XO activities with xanthine as the substrate were measured spectrophotometrically, based on the procedure reported by L. D. Kong *et al.*, with modification.¹⁶ The activity of xanthine oxidase is measured by uric acid formation monitored at 295 nm. The assay was performed in a final volume of 1 mL 50 mM K_2HPO_4 at pH 7.8 in a quartz cuvette. The reaction mixture contains 200 μL of 84.8 mg/mL xanthine in 50 mM K_2HPO_4 , 50 μL of the various concentrations tested compounds. The reaction is started by addition of 66 μL 37.7 mU/mL xanthine oxidase. The reaction is monitored for 6 min at 295 nm and the product is expressed as mmol uric acid per minute. The reactions kinetic were linear during these 6 min of monitoring.

2.4. Docking Simulations

Molecular docking study of the compounds into the 3D X-ray structure of XO (entry 1FIQ in the Protein Data Bank) was carried out by using the AutoDock version 4.2. First, AutoGrid component of the program precalculates a 3D grid of interaction energies based on the macromolecular target using the AMBER force field. The cubic grid box of $60 \times 70 \times 60 \text{ \AA}^3$ points in x , y , and z direction with a spacing of 0.375 \AA and grid maps were created representing the catalytic active target site region where the native ligand was embedded. Then automated docking studies were carried out to evaluate the binding free energy of the inhibitor within the macromolecules. The GALS search algorithm (genetic algorithm with local search) was chosen to search for the best conformers. The parameters were set using the software ADT (AutoDockTools package, version 1.5.4) on PC which is associated with AutoDock 4.2. Default settings were used with an initial population of 100 randomly placed individuals, a maximum number of 2.5×10^6 energy evaluations, and a maximum number of 2.7

$\times 10^4$ generations. A mutation rate of 0.02 and a crossover rate of 0.8 were chosen. Given the overall consideration of the most favorable free energy of binding and the majority cluster, the results were selected as the most probable complex structures.

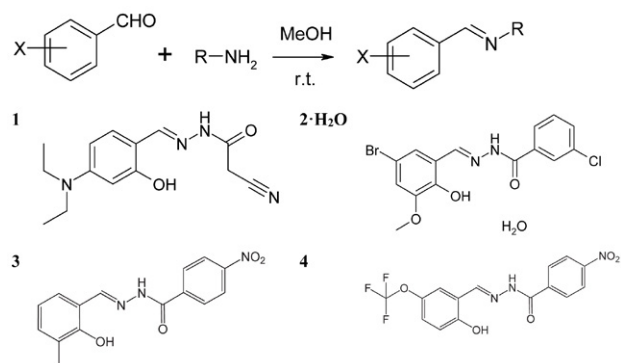
2. 5. Data Collection, Structural Determination and Refinement

Diffraction intensities for the compounds were collected at 298(2) K using a Bruker D8 VENTURE PHOTON diffractometer with Mo K α radiation ($\lambda = 0.71073$ Å). The collected data were reduced using the SAINT program,¹⁷ and multi-scan absorption corrections were performed using the SADABS program.¹⁸ The structures were solved by direct methods and refined against F^2 by full-matrix least-squares methods using the SHELXTL.¹⁹ All of the non-hydrogen atoms were refined anisotropically. The amino and water H atoms were located in difference Fourier maps and refined isotropically, with N–H, O–H and H...H distances restrained to 0.90(1), 0.85(1) and 1.37(2) Å, respectively. All other H atoms were placed in idealized positions and constrained to ride on their parent atoms. The crystallographic data for the compounds are summarized in Table 1. Hydrogen bonding information is given in Table 2.

3. Results and Discussion

3.1. Chemistry

The compounds were readily synthesized by reaction of 1:1 molar ratio of aldehydes with primary amines in methanol at room temperature (Scheme 1), with high yields (over 90%) and purity. Single crystals suitable for X-ray diffraction were obtained by slow evaporation of the solutions containing the compounds in air. The compounds have been characterized by elemental analyses and IR spectra. Structures of the compounds were further confirmed by single crystal X-ray crystallography.



Scheme 1. The synthesized hydrazones 1–4

Table 1. Crystallographic and experimental data for compounds 1–4.

Compound	1	2·H ₂ O	3	4
Formula	C ₁₄ H ₁₈ N ₄ O ₂	C ₁₅ H ₁₄ BrClN ₂ O ₄	C ₁₅ H ₁₃ N ₃ O ₄	C ₁₅ H ₁₀ F ₃ N ₃ O ₅
<i>Mr</i>	274.3	401.6	299.3	369.3
<i>T</i> (K)	298(2)	298(2)	298(2)	298(2)
Crystal system	Monoclinic	Monoclinic	Monoclinic	Monoclinic
Space group	<i>P</i> 2 ₁ / <i>c</i>	<i>P</i> 2 ₁ / <i>n</i>	<i>P</i> 2 ₁ / <i>c</i>	<i>P</i> 2 ₁ / <i>c</i>
<i>a</i> (Å)	12.582(3)	5.999(2)	11.158(1)	11.672(2)
<i>b</i> (Å)	14.562(3)	14.323(2)	13.448(1)	15.011(3)
<i>c</i> (Å)	8.389(2)	19.372(2)	9.278(1)	8.785(2)
α (°)				
β (°)	107.116(2)	96.624(2)	91.366(2)	94.744(3)
γ (°)				
<i>V</i> (Å ³)	1469.0(6)	1653.3(5)	1391.8(2)	1533.9(5)
<i>Z</i>	4	4	4	4
<i>D_c</i> (g cm ⁻³)	1.240	1.614	1.428	1.599
<i>i</i> (Mo-K α) (mm ⁻¹)	0.086	2.668	0.106	0.145
<i>F</i> (000)	584	808	624	752
Reflections collected	11691	8041	13528	14416
Unique reflections	3213	3590	2582	2697
Observed reflections ($I \geq 2\sigma(I)$)	1345	1939	2146	1471
Parameters	187	219	204	241
Restraints	1	4	1	2
Goodness-of-fit on F^2	0.999	0.999	1.055	1.028
$R_1, wR_2 [I \geq 2\sigma(I)]^a$	0.0548, 0.1269	0.0412, 0.0801	0.0424, 0.1142	0.0568, 0.1124
R_1, wR_2 (all data) ^a	0.1442, 0.1709	0.1059, 0.1006	0.0515, 0.1216	0.1358, 0.1427
Large diff. peak and hole (eÅ ⁻³)	0.202, -0.139	0.315, -0.362	0.186 and -0.146	0.331 and -0.284

^a $R_1 = F_o - F_c/F_o$, $wR_2 = [\sum w(F_o^2 - F_c^2)]/\sum w(F_o^2)]^{1/2}$

Table 2. Hydrogen bond distances (Å) and bond angles (°) for the compounds.

<i>D</i> –H... <i>A</i> (<i>D</i> –H... <i>A</i>)	<i>d</i> (<i>D</i> –H)	<i>d</i> (H... <i>A</i>)	<i>d</i> (<i>D</i> ... <i>A</i>)	Angle
1				
N3–H3...O2 ^{#1}	0.91(1)	1.98(2)	2.889(3)	172(2)
O1–H1...N2	0.82	1.90	2.631(3)	147(2)
2·H₂O				
O4–H4B...O3 ^{#2}	0.84(1)	1.96(2)	2.754(3)	158(4)
O4–H4A...O2 ^{#3}	0.84(1)	2.44(3)	3.070(4)	133(3)
O4–H4A...O1 ^{#3}	0.84(1)	2.28(2)	3.042(4)	150(4)
N2–H2...O4 ^{#4}	0.90(1)	1.96(2)	2.830(3)	162(4)
O1–H1...N1	0.82	1.86	2.580(3)	145(3)
3				
N2–H2...O2 ^{#5}	0.90(1)	2.08(1)	2.920(2)	159(2)
O1–H1...N1	0.82	1.94	2.654(2)	146
4				
O1–H1...N1	0.85(1)	1.91(2)	2.661(4)	150(4)
N2–H2...O2 ^{#6}	0.90(1)	2.02(1)	2.900(3)	166(4)

Symmetry codes: #1) $2 - x, -y, 3 - z$; #2) $1 + x, -1 + y, z$; #3) $x, -1 + y, z$; #4) $1/2 - x, 1/2 + y, 1/2 - z$; #5) $x, 1/2 - y, -1/2 + z$; #6) $x, 3/2 - y, -1/2 + z$.

3. 2. Structure Description of the Compounds

Figure 1 gives perspective view of compounds 1–4 with atomic labeling systems. X-ray crystallography reveals that the compounds are similar benzohydrazone derivatives. The asymmetric unit of compound **2·H₂O** contains a benzohydrazone molecule and a water molecule of crystallization, which is isostructural with the bromo-containing hydrazone compound 3-bromo-*N'*-(5-bromo-2-hydroxy-3-methoxybenzylidene)benzohydrazone mo-

nohydrate,²⁰ and similar to *N'*-[(*E*)-5-bromo-2-hydroxy-3-methoxybenzylidene]benzohydrazone monohydrate.²¹ All the benzohydrazone molecules of the compounds adopt *E* configuration with respect to the methyldiene units. The distances of the methyldiene bonds, ranging from 1.26 to 1.29 Å, confirm them as typical double bonds. The shorter distances of the C–N bonds and the longer distances of the C=O bonds for the –C(O)–NH– units than usual, suggest the presence of conjugation effects in the molecules. The remaining bond lengths in the

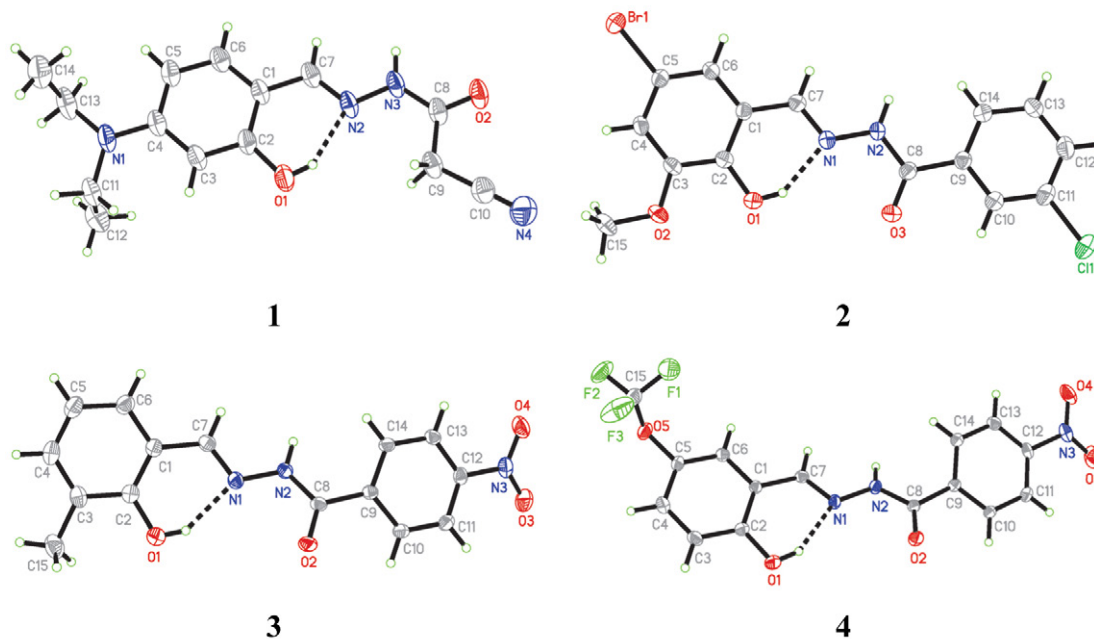


Figure 1. A perspective view of the molecular structures of the compounds 1–4 with the atom labeling scheme. Thermal ellipsoids are drawn at the 30% probability level. Hydrogen bonds are shown as dashed lines.

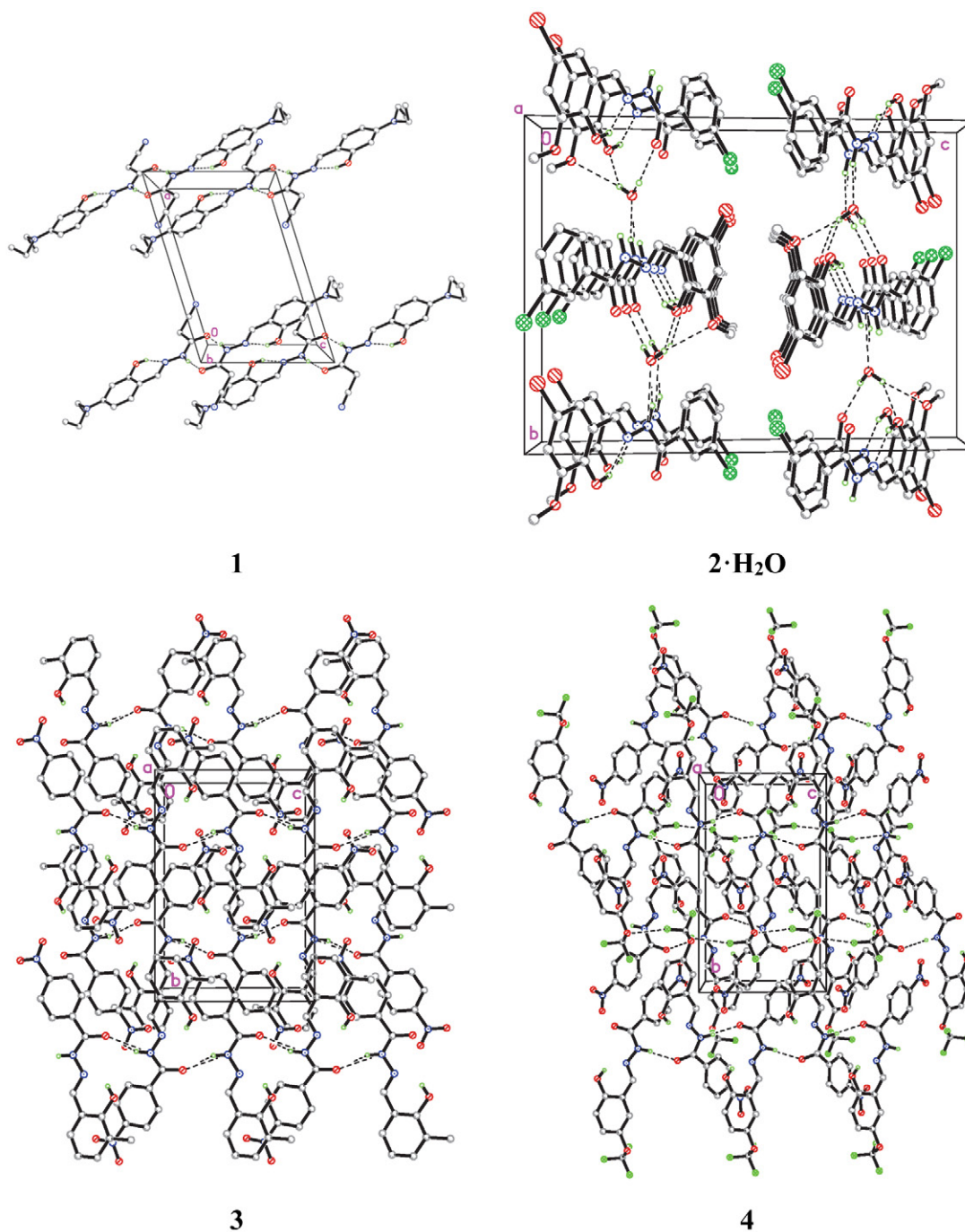


Figure 2. Molecular packing diagrams of the compounds 1–4. Hydrogen bonds are shown as dashed lines.

compounds are comparable to each other, and are within normal values.²² The dihedral angles between the two aromatic rings are $9.8(3)^\circ$ for $2 \cdot \text{H}_2\text{O}$, $12.9(5)^\circ$ for 3, and $14.9(3)^\circ$ for 4. The crystal structures of the compounds are stabilized by intermolecular hydrogen bonds (Table 2, Figure 2). As expected, the crystal packing structure of compound $2 \cdot \text{H}_2\text{O}$ is also very similar to the similar compounds mentioned above.^{13,14}

In ^1H NMR, the absence of NH_2 signals and the appearance of a peak for NH proton in the region δ

12.01–9.70 ppm and imine CH proton in the region δ 9.62–8.60 ppm confirmed the synthesis of the hydrazones. The aromatic proton signals were found in their respective regions with different multiplicities, confirming their relevant substitution pattern.

3.3. Pharmacology

The measurement of XO inhibitory activity was carried out for three parallel times. The percents of inhibition

at the concentration of 100 μM and IC_{50} values for the compounds against XO are summarized in Table 3.

Table 3. Inhibition of XO by the tested materials.

Tested materials	Percent of inhibition ^b	IC_{50} (μM)
1	74.0 \pm 3.3	15.8 \pm 1.5
2	44.5 \pm 2.8	—
3	25.5 \pm 2.0	—
4	31.2 \pm 1.7	—
Allopurinol	80.7 \pm 4.3	8.7 \pm 2.3

^bThe concentration of the tested material is 100 μM .

Allopurinol was used as a reference with the percent of inhibition of 80.7 \pm 4.3 and with IC_{50} value of 8.7 \pm 2.3 μM . Compound **1** shows the most effective activity with the percent of inhibition of 74.0 \pm 3.3 and with IC_{50} value of 15.8 \pm 1.5 μM . Although the number of tested compounds is limited, some structural features, important to the xanthine oxidase inhibitory effect, can be inferred. The merely difference of compounds **3** and **4** is the substituent groups of the benzene rings, *viz.* CH_3 for **3** and OCF_3 for **4**. As a result, the XO inhibitory activity of **3** is less than **4**. Detailed investigation of the structure-activity relationship reveals that the presence of Cl and Br substituent groups may contribute to the inhibition, which is revealed by compound **2**. These findings are coherent with the results reported in the literature that the presence of electron-withdrawing groups in the benzene rings can enhance the activities,²³ and also comparable to that compounds with the presence of bulky ethyl group have stronger activity than those bearing methyl group.²⁴ As a comparison, compound **1** has stronger activity than the Schiff base copper complexes,^{14b} and the OH and Br substituted hydrazone compounds,²⁶ but lower activity than *N*-(3-cyano-1*H*-indol-5/6-yl)-6-oxo-1,6-dihydropyrimidine-4-carboxamides and 5-(6-oxo-1,6-dihydropyrimidin-2-yl)-1*H*-indole-3-carbonitriles,⁸

N-(3-cyano-1-cyclopentyl-1*H*-indol-5-yl)-1*H*-benzo[*d*]imidazole-5-carboxamide,⁹ and the Cl and CN substituted hydrazone compounds.^{14b}

3. 4. Molecular Docking Study

In order to give an explanation and understanding of potent inhibitory activity observed from the experiment, molecular docking study was performed to investigate the binding effects between the compound **1** and the active sites of XO (entry 1FIQ in the Protein Data Bank). Allopurinol was used to verify the model of docking, and gave satisfactory results. Figure 3 is the binding model for the compound **1** in the enzyme active site of XO. The docking score is -7.12 . As a comparison, the docking score for Allopurinol is -6.27 .

From the docking results, it can be seen that the molecule of compound **1** is well filled in the active pocket of XO. The molecule of **1** binds with the enzyme through four hydrogen bonds with Ser876, Ala1011 and Thr1010. In addition, there exist hydrophobic interactions among the compounds with the active sites of the enzyme. The results of the molecular docking study could explain the effective inhibitory activity of compound **1** on XO.

4. Conclusion

The present study reports the synthesis, crystal structures and XO inhibitory activities of a series of hydrazones. The compounds were characterized by elemental analysis, IR and ¹H NMR spectra, as well as single crystal X-ray diffraction. Among the compounds, 2-cyano-*N*'-(4-diethylamino-2-hydroxybenzylidene) acetohydrazide has effective XO inhibition with IC_{50} value of 15.8 \pm 1.5 μM , which may be used as a potential XO inhibitor, and deserves further study. The molecule of the compound can be well filled and combined with hydrogen bonds in the active pocket of XO.

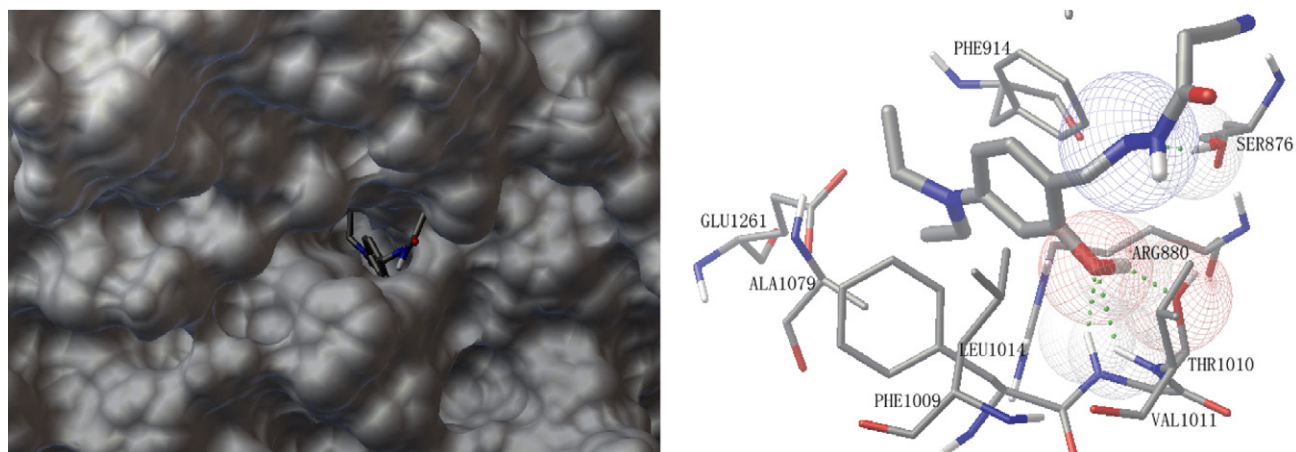


Figure 3. 3D (left) and 2D (right) binding mode of **1** with the active site of XO. Hydrogen bonds are shown as dashed lines.

Supplementary Material

CCDC – 892363 for **1**, 892364 for **2·H₂O**, 1041580 for **3**, and 1041581 for **4** contain the supplementary crystallographic data for this article. These data can be obtained free of charge at <http://www.ccdc.cam.ac.uk/const/retrieving.html> or from the Cambridge Crystallographic Data Centre (CCDC), 12 Union Road, Cambridge CB2 1EZ, UK; fax: +44(0)1223-336033 or e-mail: deposit@ccdc.cam.ac.uk.

5. References

- (a) R. Roncato, J. Angelini, A. Pani, E. Cecchin, A. Sartore-Bianchi, S. Siena, E. de Mattia, F. Scaglione, G. Toffoli, *Inter. J. Mol. Sci.* **2020**, *21*, 6350; DOI:10.3390/ijms21176350
(b) S. Kaur, Y. Bansal, R. Kumar, G. Bansal, *Bioorg. Med. Chem.* **2020**, *28*, 115327; DOI:10.1016/j.bmc.2020.115327
(c) D. W. Banner, P. Hadvary, *J. Biol. Chem.* **1991**, *266*, 20085–20093; DOI:10.1016/S0021-9258(18)54894-8
(d) E. Sandstrom, *Drugs* **1989**, *38*, 417–450. DOI:10.2165/00003495-198938030-00005
- (a) T. Mori, H. Muramatsu, T. Matsui, A. McKee, T. Asano, *Neuropath. Appl. Neurobiol.* **2000**, *26*, 31–40; DOI:10.1046/j.1365-2990.2000.00215.x
(b) A. Pinto, M. Kornfeld, H. Aubin, P. Akhyari, A. Lichtenberg, *Free Rad. Biol. Med.* **2014**, *76*, S52–S52; DOI:10.1016/j.freeradbiomed.2014.10.420
(c) L. Tian, R. Belardinelli, P. Carnevali, F. Principi, G. Seddaiu, G. P. Littarru, *Eur. Heart J.* **2007**, *28*, 2249–2255; DOI:10.1093/eurheartj/ehm267
(d) P. H. Chan, J. W. Schimidley, R. A. Fishman, S. M. Longar, *Neurology* **1984**, *34*, 315–320. DOI:10.1212/WNL.34.3.315
- (a) E. O. Dangana, T. E. Omolekulo, E. D. Areola, K. S. Olaniyi, A. O. Soladoye, L. A. Olatunji, *Chem. Biol. Interact.* **2020**, *316*, 108929; DOI:10.1016/j.cbi.2019.108929
(b) Y. Q. Wu, H. He, T. Hou, *J. Food Sci.* **2021**, *86*, 1081–1088; DOI:10.1111/1750-3841.15603
(c) X. Yu, L. Zhang, P. Zhang, J. Zhi, R. N. Xing, L. Q. He, *Pharm. Biol.* **2020**, *58*, 944–949; DOI:10.1080/13880209.2020.1817951
(d) J. Nomura, N. Busso, A. Ives, C. Matsui, S. Tsujimoto, T. Shirakura, M. Tamura, T. Kobayashi, A. So, Y. Yamanaka, *Sci. Rep.* **2014**, *4*, 4554; DOI:10.1038/srep04554
(e) M. M. Kolomiets, A. Bilchenko, *Eur. J. Heart Fail.* **2019**, *21*, 356–356;
(f) B. Butts, D. A. Calhoun, T. S. Denney, S. G. Lloyd, H. Gupta, K. K. Gaddam, I. Aban, S. Oparil, P. W. Sanders, R. Patel, J. F. Collawn, L. J. Dellitalia, *Free Rad. Biol. Med.* **2019**, *134*, 343–349; DOI:10.1016/j.freeradbiomed.2019.01.029
(g) P. Pacher, A. Nivorozhkin, C. Szabo, *Pharmacol. Rev.* **2006**, *58*, 87–114; DOI:10.1124/pr.58.1.6
(h) A. A. Fatokun, T. W. Stone, R. A. Smith, *Neurosci. Lett.* **2007**, *416*, 34–38. DOI:10.1016/j.neulet.2007.01.078
- (a) P. C. Robinson, N. Dalbeth, P. Donovan, *Arthr. Care Res.* **2021**, *73*, 1537–1543; DOI:10.1002/acr.24357
(b) C. A. Hay, J. A. Prior, J. Belcher, C. D. Mallen, E. Roddy, *Arthr. Care Res.* **2021**, *73*, 1049–1054; DOI:10.1002/acr.24205
(c) S. Z. Zhang, T. Xu, Q. Y. Shi, S. Y. Li, L. Wang, Z. M. An, N. Su, *Front. Med.* **2021**, *8*, 698437; DOI:10.3389/fmed.2021.698437
(d) L. G. Gao, B. Wang, Y. Pan, Y. Lu, R. Cheng, *Clin. Cardiol.* **2021**, *44*, 907–916;
(e) A. Jeyaruban, W. Hoy, A. Cameron, H. Healy, Z. Wang, J. Zhang, A. Mallett, *J. Nephrol.* **2021**, *34*, 753–762; DOI:10.1007/s40620-020-00937-4
(f) T. Novinsion, B. Bhooshan, T. Okabe, G. R. Revankar, R. K. Robins, K. Senga, H. R. Wilson, *J. Med. Chem.* **1976**, *19*, 512–516. DOI:10.1021/jm00226a013
- K. Okamoto, B. T. Eger, T. Nishino, E. F. Pai, T. Nishino, *Nucleos. Nucleot. Nucl. Acids* **2008**, *27*, 888–893. DOI:10.1080/15257770802146577
- (a) A. Smelcerovic, K. Tomovic, Z. Smelcerovic, Z. Petronijevic, G. Kocic, T. Tomasic, Z. Jakopin, M. Anderluh, *Eur. J. Med. Chem.* **2007**, *135*, 491–516;
(b) G. Beyer, M. F. Melzig, *Biol. Pharm. Bull.* **2005**, *28*, 1183–1186; DOI:10.1248/bpb.28.1183
(c) A. Haberland, H. Luther, I. Schinker, *Agents Actions* **1991**, *32*, 96–97. DOI:10.1007/BF01983326
- (a) J. X. Zhao, Q. Mao, F. W. Lin, B. Zhang, M. Sun, T. J. Zhang, S. J. Wang, *Eur. J. Med. Chem.* **2022**, *229*, 114086;
(b) N. Zhai, C. C. Wang, F. S. Wu, L. W. Xiong, X. G. Luo, X. L. Ju, G. Y. Liu, *Inter. J. Mol. Sci.* **2021**, *22*, 8122. DOI:10.3390/ijms22158122
- (a) T.-J. Zhang, S. Tu, X. Zhang, Q.-Y. Wang, S.-S. Hu, Y. Zhang, Z.-H. Zhang, Z.-R. Wang, F.-H. Meng, *Bioorg. Chem.* **2021**, *117*, 105417; DOI:10.1016/j.bioorg.2021.105417
(b) B. Zhang, Y. L. Duan, Y. W. Yang, Q. Mao, F. W. Lin, J. Gao, X. W. Dai, P. Zhang, Q. H. Li, J. X. Li, R. H. Dai, S. J. Wang, *Eur. J. Med. Chem.* **2022**, *227*, 113928.
- S. Tu, T.-J. Zhang, Y. Zhang, X. Zhang, Z.-H. Zhang, F.-H. Meng, *Bioorg. Chem.* **2021**, *115*, 105181.
- A. Alsayari, M. Z. Hassan, Y. I. Asiri, A. Bin Muhsinah, M. Kamal, M. S. Akhtar, *Indian J. Heterocycl. Chem.* **2021**, *31*, 635–640.
- J. L. Serrano, D. Lopes, M. J. A. Reis, R. E. F. Boto, S. Silvestre, P. Almeida, *Biomedicines* **2021**, *9*, 1443. DOI:10.3390/biomedicines9101443
- H. Hayun, R. Hanifati, A. D. Pratiwik, *Indian J. Pharm. Sci.* **2021**, *83*, 1074–1080.
- (a) M. Kaur, S. Kumar, M. Yusuf, J. Lee, R. J. C. Brown, K. H. Kim, A. K. Malik, *Coord. Chem. Rev.* **2021**, *449*, 214214; DOI:10.1016/j.ccr.2021.214214
(b) G.-X. He, L.-W. Xue, Q.-L. Peng, P.-P. Wang, H.-J. Zhang, *Acta Chim. Slov.* **2019**, *66*, 570–575; DOI:10.17344/acsi.2018.4868
(c) C.-L. Zhang, X.-Y. Qiu, S.-J. Liu, *Acta Chim. Slov.* **2019**, *66*, 484–489; DOI:10.17344/acsi.2019.5019
(d) J. Qin, Q. Yin, S.-S. Zhao, J.-Z. Wang, S.-S. Qian, *Acta Chim. Slov.* **2016**, *53*, 55–61; DOI:10.17344/acsi.2015.1918

- (e) F. Qureshi, M. Y. Khuhawar, T. M. Jahangir, A. H. Chanar, *Acta Chim. Slov.* **2016**, *63*, 113–120; DOI:10.17344/acsi.2015.1994
- (f) X.-Q. Luo, Q.-R. Liu, Y.-J. Han, L.-W. Xue, *Acta Chim. Slov.* **2020**, *67*, 159–166; DOI:10.17344/acsi.2019.5303
- (g) K. M. El-Mahdy, A. M. E.-Kazak, M. Abdel-Megid, M. Seada, O. Farouk, *Acta Chim. Slov.* **2016**, *67*, 18–25. DOI:10.17344/acsi.2015.1555
14. (a) N. Choudhary, D. L. Hughes, U. Kleinkes, L. F. Larkworthy, G. J. Leigh, M. Maiwald, C. J. Marmion, J. R. Sanders, G. W. Smith, C. Sudbrake, *Polyhedron* **1997**, *16*, 1517–1528; DOI:10.1016/S0277-5387(96)00436-6
(b) M. Leigh, C. E. Castillo, D. J. Raines, A. K. Duhme-Klair, *ChemMedChem* **2011**, *6*, 612–616. DOI:10.1002/cmdc.201000429
15. (a) Y. Lu, D.-H. Shi, Z.-L. You, X.-S. Zhou, K. Li, *J. Coord. Chem.* **2012**, *65*, 339–352; DOI:10.1080/00958972.2011.653785
(b) D. Qu, F. Niu, X. Zhao, K.-X. Yan, Y.-T. Ye, J. Wang, M. Zhang, Z. You, *Bioorg. Med. Chem.* **2015**, *23*, 1944–1949. DOI:10.1016/j.bmc.2015.03.036
16. L.D. Kong, Y. Zhang, X. Pan, R. X. Tan, C. H. K. Cheng, *Cell Mol. Life Sci.* **2000**, *57*, 500–505. DOI:10.1007/PL00000710
17. Bruker, SMART and SAINT. Bruker AXS Inc., Madison, Wisconsin, USA (2002).
18. G. M. Sheldrick, SADABS. Program for Empirical Absorption Correction of Area Detector, University of Göttingen, Germany (1996).
19. G. M. Sheldrick, *Acta Crystallogr.* **2008**, *A64*, 112–122. DOI:10.1107/S0108767307043930
20. H.-Y. Zhu, *Asian J. Chem.* **2012**, *24*, 558–560.
21. J. Emmanuel, M. Sithambaresan, M. R. Prathapachandra Kurup, *Acta Crystallogr.* **2013**, *E69*, o1775–o1776. DOI:10.1107/S1600536813030572
22. (a) F. H. Allen, O. Kennard, D. G. Watson, L. Brammer, A. G. Orpen, R. Taylor, *J. Chem. Soc. Perkin Trans.* **1987**, *2*, S1–19;
(b) M. Zhang, D.-M. Xian, H.-H. Li, J.-C. Zhang, Z.-L. You, *Aust. J. Chem.* **2012**, *65*, 343–350; DOI:10.1071/CH11424
(c) F.-M. Wang, L.-J. Li, G.-W. Zang, T.-T. Deng, Z.-L. You, *Acta Chim. Slov.* **2021**, *68*, 541–547; DOI:10.17344/acsi.2020.6051
(d) G.-X. He, L.-W. Xue, *Acta Chim. Slov.* **2021**, *68*, 567–574; DOI:10.17344/acsi.2020.6333
(e) H.-Y. Zhu, *Acta Chim. Slov.* **2021**, *68*, 65–71.
23. S. Gupta, L. M. Rodrigues, A. P. Esteves, A. M. F. Oliveira-Campos, M. S. J. Nascimento, N. Nazareth, H. Cidade, M. P. Neves, E. Fernandes, M. Pinto, N. M. F. S. A. Cerqueira, N. Bras, *Eur. J. Med. Chem.* **2008**, *43*, 771–780. DOI:10.1016/j.ejmech.2007.06.002
24. S. Wang, J. Yan, J. Wang, J. Chen, T. Zhang, Y. Zhao, M. Xue, *Eur. J. Med. Chem.* **2010**, *45*, 2663–2670. DOI:10.1016/j.ejmech.2010.02.013
25. Y.-Q. Cui, Z.-L. You, X.-F. Li, X.-L. Wang, Y.-P. Ma, C. Wang, C.-L. Zhang, *Transition Met. Chem.* **2010**, *35*, 159–163. DOI:10.1007/s11243-009-9309-6

Povzetek

Sintetizirali smo serijo hidrazonov: 2-ciano-*N'*-(4-dietilamino-2-hidroksibenziliden)acetohidrazid (**1**), *N'*-(5-bromo-2-hidroksi-3-metoksibenziliden)-3-klorobenzohidrazid monohidrat (**2**·H₂O), *N'*-(2-hidroksi-3-metilbenziliden)-4-nitrobenzohidrazid (**3**) in *N'*-(2-hidroksi-3-trifluorometoksibenziliden)-4-nitrobenzohidrazid (**4**). Pripravljene spojine smo strukturno karakterizirali z elementno analizo, IR in ¹H NMR spektroskopijo ter rentgensko difrakcijo na monokristalu. Preučili smo tudi inhibitorno aktivnost proti ksantin oksidazi. Izmed vseh spojin se je 2-ciano-*N'*-(4-dietilamino-2-hidroksibenziliden)acetohidrazid izkazal kot najbolj učinkovit. Da bi ugotovili verjetne načine vezave preučevanih hidrazonov v aktivno mesto ksantin oksidaze, smo izvedli tudi molekulsko sidranje spojin v kristalno strukturo tega encima.



Except when otherwise noted, articles in this journal are published under the terms and conditions of the Creative Commons Attribution 4.0 International License